

## Two-photon anisotropy: Analytical description and molecular modeling for symmetrical and asymmetrical organic dyes

Jie Fu <sup>a,\*</sup>, Olga V. Przhonska <sup>a,c</sup>, Lazaro A. Padilha <sup>a,d</sup>, David J. Hagan <sup>a,b</sup>,  
Eric W. Van Stryland <sup>a,b</sup>, Kevin D. Belfield <sup>a,e</sup>, Mikhail V. Bondar <sup>c,e</sup>,  
Yuriy L. Slominsky <sup>f</sup>, Alexei D. Kachkovski <sup>f</sup>

<sup>a</sup> College of Optics and Photonics: CREOL & FPCE, University of Central Florida, 4000 Central Florida Boulevard, Orlando, FL 32816, USA

<sup>b</sup> Department of Physics, University of Central Florida, Orlando, FL 32816, USA

<sup>c</sup> Institute of Physics, National Academy of Sciences, Prospect Nauki 46, Kiev 03028, Ukraine

<sup>d</sup> Instituto de Física “Gleb Wataghin”, Universidade Estadual de Campinas, P.O. Box 6165, Brazil 13083-970, USA

<sup>e</sup> Department of Chemistry, University of Central Florida, Orlando, FL 32816, USA

<sup>f</sup> Institute of Organic Chemistry, National Academy of Sciences, Murmanskaya 5, Kiev 03094, Ukraine

Received 23 May 2005; accepted 18 August 2005

Available online 28 September 2005

### Abstract

One- and two-photon anisotropy spectra of a series of symmetrical and asymmetrical polymethine (PD) and fluorene molecules were measured experimentally and discussed theoretically within the framework of three-state and four-state models. For all the molecules discussed in this paper, the experimental two-photon anisotropy values,  $r_{2PA}$ , lie in the relatively narrow range from 0.47 to 0.57 and remain almost independent of wavelength over at least two electronic transitions. This is in contrast with their one-photon anisotropy, which shows strong wavelength dependence, typically varying from  $\approx 0$  to 0.38 over the same transitions. A detailed analysis of the two-photon absorption (2PA) processes allows us to conclude that a three-state model can explain the 2PA anisotropy spectra of most asymmetrical PDs and fluorenes. However, this model is inadequate for all the symmetrical molecules. Experimental values of  $r_{2PA}$  for symmetrical polymethines and fluorenes can be explained by symmetry breaking leading to the deviation of the orientation of the participating transition dipole moments from their “classical” orientations.

© 2005 Elsevier B.V. All rights reserved.

**Keywords:** Polymethine dyes; Fluorenes; Two-photon absorption; One- and two-photon anisotropy; Transition dipole moments; Symmetry breaking

### 1. Introduction

The development of new organic materials for two-photon absorption (2PA) is an ongoing area of research. Even though there has been considerable progress in the studies of structure–property relationships of organic molecules, much more remains to be discovered. Polymethine (PDs) dyes are attractive candidates for 2PA studies due to their very large ground-state transition dipole moments, close to parallel orientation of their ground- and excited state tran-

sitions [1], and sharp low-energy side of their linear absorption spectra allowing significant intermediate state resonance enhancement of the 2PA [2]. Recent studies from various research groups have shown design strategies for efficient 2PA by a systematic investigation of the conjugation length of the chromophores, various symmetrical and asymmetrical combinations of electron–donor and electron–acceptor terminal groups, and the addition of such groups in the middle of the chromophore to vary the charge distribution [3–7].

A much less investigated approach for understanding the 2PA properties of organic molecules is the study of the spectral dependence of the one-photon and two-photon

\* Corresponding author. Tel.: +1 407 823 6866; fax: +1 407 823 6880.  
E-mail address: [jfu@creol.ucf.edu](mailto:jfu@creol.ucf.edu) (J. Fu).

anisotropy. The first theoretical studies related to this subject were published independently by Callis [8], Johnson [9] and der Meer [10] and are based on the treatment of the 2PA tensor with the addition of the fluorescence transition dipole. A theoretical approach presented by Callis for the steady-state two-photon anisotropy, is used by us in Section 3 and extended for three- and four-level molecular models. Johnson and Van der Meer were more concerned with the theoretical investigation of two-photon anisotropy decay in isotropic [9] or oriented [10] systems. In contrast, our goal is to obtain a practical expression for the steady-state two-photon anisotropy that may be used to model the experimental anisotropy spectra. Such studies can give additional information about the nature of intermediate states and the molecular symmetry. It is commonly known that one-photon anisotropy measurements, especially linked to quantum-chemical calculations, can reveal the spectral positions and orientations of the transition dipole moments from the ground to the first excited state,  $\mu_{01}$ , and higher excited-states,  $\mu_{0n}$ , relative to the orientation of the emission dipole moment,  $\mu_{10}$ . This cannot be obtained from one-photon absorption spectra. For polymethines, one-photon anisotropy values,  $r_{1PA}$ , within the first absorption band are typically close to the theoretical maximum of 0.4, indicating that  $\mu_{01}$  is parallel to  $\mu_{10}$ . In this case, one-photon anisotropy measurements determine the mutual orientation of different absorbing dipoles that is important for understanding 2PA processes. It was shown theoretically [8,10] that the range of two-photon anisotropy,  $r_{2PA}$ , values is much broader than for  $r_{1PA}$  (from  $-0.32$  to  $0.61$ ) indicating potential advantages of two-photon excitation. In practice, as will be shown in this paper and in a previous paper [11],  $r_{2PA}$  spectra for many organic dyes are almost wavelength independent within several electronic transitions. It is necessary to note that  $r_{2PA}$  studies are very limited. Most of the measurements were performed only within one electronic band, and their analysis is usually directed at a comparison of the values of  $r_{1PA}$  and  $r_{2PA}$ . An overview of the existing experimental data were presented by Lakowicz and Gryczynski in [12] (see also references therein). However, to our knowledge, an explanation of the wavelength independent behavior of  $r_{2PA}$  as well as its potential for understanding the properties of 2PA have not yet been reported.

In this paper, the one- and two-photon anisotropy spectra of a series of symmetrical and asymmetrical polymethine and fluorene molecules are reported and analyzed theoretically in the framework of a three-state model with one-intermediate-level and a four-state model with two-intermediate-levels. This allows us to reveal the reasons for the unusual behavior of  $r_{2PA}$  and provides a deeper insight into the nature of 2PA processes. In the following sections, we will describe (1) the structure and one-photon absorption properties of two symmetrical and two asymmetrical PDs, and symmetrical and asymmetrical fluorene molecules; (2) the techniques used for  $r_{2PA}$  measurements; (3) a derivation of  $r_{2PA}$  formulas for a four-state model

and a simplified three-state model; and (4) molecular modeling, using the results of quantum-chemical calculations for the analysis of the 2PA processes in these dyes.

## 2. Experimental

### 2.1. Materials

The molecular structures of the dyes (polymethines and fluorenes) studied in this paper are shown in Fig. 1. Their chemical names are: 2-[5-(1,3-dihydro-3,3-dimethyl-1-propyl-2H-indol-2-ylidene)-1,3-pentadienyl]-3,3-dimethyl-1-propylindolium iodide (labeled as PD 2350); 3,3,3,3-tetramethyl-1,1-diphenylindotricarbocyanine perchlorate (labeled as PD 3428); 2-[5-(1,3-dihydro-1,3,3-trimethyl-2H-indol-2-ylidene)-1,3-pentadienyl]-3-ethyl-1,3-benzothiazolium perchlorate (labeled as PD 2665); 2-[(E)-2-(4-dimethylaminophenyl)-1-ethenyl]-3-methyl-1,3-benzothiazolium *p*-toluene sulfonate (Styryl 1); *N*-(7-benzothiazol-2-yl-9,9-bis-decyl-9H-fluoren-2-yl)-acetamide (fluorene 1) and 9,9-didecyl-2,7-bis-(*N,N*-benzothiazoyl) fluorene (fluorene 2). The main spectroscopic properties

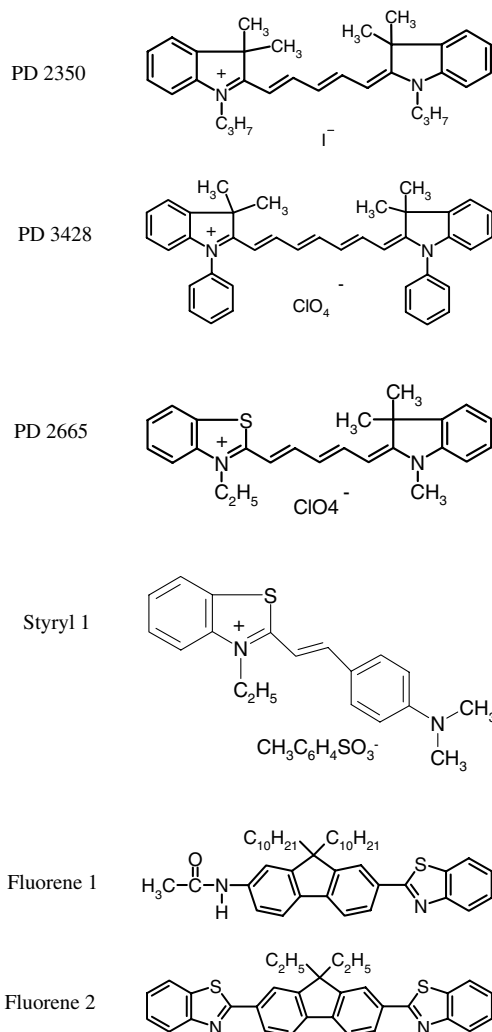


Fig. 1. Molecular structures.

of the cationic PDs are determined by the existence of a delocalized  $\pi$ -electron system in the polymethine chromophore (or polymethine chain) and symmetric (PDs 2350 and 3428) or asymmetric (PD 2665 and Styryl 1) terminal groups, which also possess a delocalized  $\pi$ -electron system. PD 2665 can be considered as a weakly asymmetrical dye (Donor –  $\pi$  conjugation – Donor) with the terminal groups of almost equal electron-donor abilities. In contrast, Styryl 1 is a strongly asymmetrical dye with a Donor –  $\pi$  conjugation – Acceptor (benothiazolyl) structure. These PDs were synthesized at the Institute of Organic Chemistry, Kiev, Ukraine, by standard methods as described in [13]. Both fluorene molecules with symmetrical (fluorene 2) and asymmetrical (fluorene 1) structures represent Acceptor – aromatic fluorene core – Acceptor systems. The rigid ring structure of the fluorene core is responsible for the high thermal and photochemical stability, as well as for the efficient fluorescence nature. Synthesis of fluorene dyes 1 and 2 was performed at the Chemistry Department of the University of Central Florida, Orlando, USA, and is described in [14,15]. The molecular structures of all dyes were confirmed by elemental analysis and nuclear magnetic resonance spectra. The linear absorption spectra for all dyes were recorded with a Varian Cary 500 spectrophotometer, and are presented in Fig. 2. As can be seen, fluorenes 1 and 2 absorb in the shortest wavelength region, 300–400 nm. A broad absorption band with the peak position at 527 nm belongs to Styryl 1 in ethanol. The absorption spectrum of the weakly asymmetrical PD 2665 almost overlaps the spectrum of its symmetrical analogue PD 2350 but is broader, which is typical for asymmetric dyes. An increase in the length of the polymethine chromophore to one chain in PD 3428 leads to a red shift in the peak position of about 100 nm as compared to PD 2350. The extinction coefficients at the absorption peaks are:  $0.65 \times 10^5$  and  $0.31 \times 10^5 \text{ M}^{-1} \text{ cm}^{-1}$  in THF for fluorenes 1 and 2, respectively;  $0.62 \times 10^5$ ,  $2 \times 10^5$ ,  $2.36 \times 10^5$  and  $2.9 \times 10^5 \text{ M}^{-1} \text{ cm}^{-1}$  in ethanol for Styryl 1, and PDs 2665, 2350 and 3428, respectively.

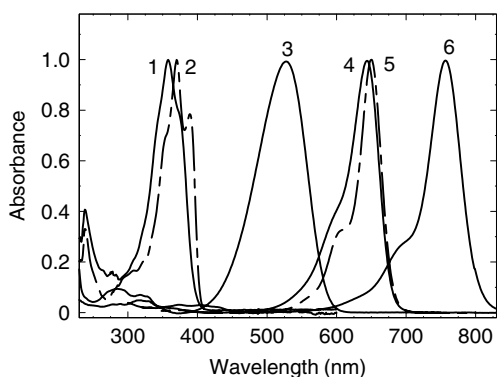


Fig. 2. Linear absorption spectra of fluorene 1 (1), fluorene 2 (dashed line 2) in THF, Styryl 1 (3), PD 2665 (4), PD 2350 (dashed line 5) and PD 3428 (6) in ethanol.

## 2.2. Experimental methods

Steady-state one-photon fluorescence and excitation anisotropy spectra of organic dyes were measured in high viscosity solvents (glycerol for PDs and *p*-THF for fluorenes) to avoid reorientation, and in low concentration solutions ( $C \approx 10^{-6} \text{ M}$ ) to avoid reabsorption, with a PTI Quantamaster Spectrofluorimeter. It is well-known that the excitation anisotropy spectrum,  $r(\lambda)$ , can be calculated as a function of the excitation wavelength  $\lambda$  at a fixed emission wavelength, usually near a fluorescence maximum:  $r(\lambda) = \frac{I_{\parallel}(\lambda) - I_{\perp}(\lambda)}{I_{\parallel}(\lambda) + 2I_{\perp}(\lambda)}$ , where  $I_{\parallel}$  and  $I_{\perp}$  are the fluorescence intensities polarized parallel and perpendicular to the excitation light [16]. One-photon anisotropy measurements can give information about the spectral position and orientation of the transition dipole moments from the ground ( $S_0$ ) to the first ( $S_1$ ) and higher ( $S_n$ ) excited-states relative to the orientation of the emission dipole moment. The angle between the absorption and emission dipole moments ( $\beta$ ) can be determined from one-photon anisotropy,  $r_{1\text{PA}} = \frac{3\cos^2\beta - 1}{2}$ . In the range:  $0^\circ \leq \beta \leq 90^\circ$ , one-photon anisotropy ranges between,  $-0.2 \leq r_{1\text{PA}} \leq 0.4$ .

Two-photon anisotropy measurements were performed using linear polarized excitation from a Clark-MXR, CPA2010, Ti:Sapphire amplified system followed by an optical parametric generator/amplifier (model TOPAS 4/800, Light Conversion) providing laser pulses of 140 fs (FWHM) duration with 1 kHz repetition rate. The tuning range is 520–2100 nm (0.6–2.38 eV). This femtosecond laser system was also used for 2PA spectra measurements. Up-converted fluorescence of all molecules under two-photon excitation was measured in 10 mm quartz cuvettes with the same PTI Quantamaster Spectrofluorimeter. Special care was taken to minimize reabsorption of the emission, especially for the dyes with a small Stokes shift as, for example, for PDs with a typical Stokes shift of  $\approx 15$ –20 nm. We controlled this reabsorption by comparing the shapes of up-converted fluorescence (usually red-shifted due to the high concentration typically used for 2PA studies) with one-photon fluorescence obtained from solutions diluted to  $\approx 10^{-6} \text{ M}$ . We found experimentally that for all the molecules studied the up-converted fluorescence at concentrations  $\leq 10^{-5} \text{ M}$  completely overlaps the one-photon fluorescence band confirming that reabsorption is negligible. Therefore, we used  $10^{-5} \text{ M}$  or smaller concentrations for all two-photon anisotropy studies. The measurements and calculations of  $r_{2\text{PA}}$  were performed as described above for  $r_{1\text{PA}}$ .

Frequency degenerate 2PA spectra of the sample solutions were measured by two methods: single-wavelength, open aperture Z-scan and up-converted fluorescence [17]. In both experiments we used the femtosecond parametric generator/amplifier described above. The Z-scans allow the determination of 2PA cross-sections from fitting procedure. This method was mainly applied for the measurements within the stronger second allowed 2PA-band. The

more sensitive method of up-converted fluorescence was applied to measure a weak 2PA-band within the first linear absorption band which is forbidden for 2PA of the symmetrical molecules by symmetry rules. Fluorescence quantum yields of PDs and fluorenes in solutions were measured using a standard method [17] relative to Rhodamine 6G (0.96 in ethanol) [18] and 9,10-diphenylanthracene (0.95 in cyclohexane) [16]. 2PA cross-sections for PDs were measured and calibrated against well-known reference standards: Fluorescein in water (pH 11) and Rhodamine B in methanol [17]. Experimental results for two-photon anisotropy and 2PA spectra are shown and discussed in the Section 4.

### 2.3. Methodology of quantum-chemical calculations

Quantum-chemical calculations of polymethines and fluorenes were performed with the goal of understanding the unusual spectral behavior of  $r_{2PA}$  as compared to  $r_{1PA}$  and revealing the best computational models. The equilibrium molecular geometry and the charge distribution in the ground state were calculated employing the semi-empirical Hartree–Fock Austin Model 1 (AM1) method as implemented into the MOPAC package with gradient  $<0.01$  kcal mol $^{-1}$ . It was demonstrated previously that the charges and C–C bond lengths calculated in this method are in good agreement with the corresponding values calculated by an ab initio method [19]. Additionally, the charge distribution and electron transition energies were calculated in INDO/S and PPP (Parr–Pariser–Pople) approximations (with the spectral parameterization) using all  $\pi \rightarrow \pi^*$  singly excited configurations. It was found that the amplitudes of the charges are different for the different methods; however, all methods predict the same trends in the behavior of the charge distribution. All calculations were performed on isolated molecules neglecting solvent effects. We calculated the permanent ground and excited-state dipoles, the transition dipole moments and their mutual orientations for both symmetrical and asymmetrical PDs and fluorenes which are all necessary for computing  $r_{2PA}$  as will be discussed below in more detail.

### 3. Theory: Derivation of two-photon anisotropy for a four-state model

The following derivation of the two-photon anisotropy formula is based on two theoretical approaches. The first by Callis [8], used a general treatment for the 2PA tensor, based on second-order perturbation theory, with the addition of the fluorescence transition dipole to develop the equation for the two-photon anisotropy. The second theoretical approach by Cronstrand et al. [20], derived an equation for the 2PA cross-section in a more specific four-state, two-intermediate-level model taking into account the influence of two excitation channels. This second model did not address fluorescence. Here, we use

Cronstrand et al.'s more detailed model of the 2PA tensor in Callis' treatment to obtain a practical model for two-photon fluorescence anisotropy that we may use to model our experiments.

Following Callis [8], the two-photon anisotropy,  $r_{2PA}$ , can be written as

$$r_{2PA} = \frac{18Q_x + Q_y - 7}{7Q_y + 14}, \quad (1)$$

where  $Q_x$  and  $Q_y$  are functions depending on the 2PA tensor  $\mathbf{S}$  and the fluorescence transition dipole  $\mathbf{F}$ :

$$Q_x = f_x^2 s_{xx}^2 + 2f_x s_{xx} f_y s_{xy} + f_y^2 s_{xy}^2 + f_x^2 s_{xy}^2 + 2f_x s_{xy} f_y s_{yy} + f_y^2 s_{yy}^2$$

and  $Q_y = (s_{xx} + s_{yy})^2,$  (2)

where  $f_x, f_y$  and  $s_{xx}, s_{xy}, s_{yy}$  are normalized matrix elements of  $\mathbf{S}$  and  $\mathbf{F}$ . Here, and below for simplicity we consider the two-dimensional approximation (case of a planar molecule placed in the  $x$ – $y$  plane), linear polarization of the excitation light, two identical photons and steady-state condition with completely motionless molecules.

Substituting (2) into (1) gives an expression for  $r_{2PA}$ :

$$r_{2PA} = \frac{2}{7} \left[ \frac{9(f_x^2 s_{xx} + 2f_x f_y s_{xy} + f_y^2 s_{yy})(s_{xx} + s_{yy}) - 4(s_{xx} + s_{yy})^2 + 1}{(s_{xx} + s_{yy})^2 + 2} \right]. \quad (3)$$

This is a general formula for the steady-state two-photon anisotropy, which is valid for any number of states. In order to derive an equation for  $r_{2PA}$ , which can be practically applied for the analysis of real molecules, we need to choose an adequate molecular model and connect the normalized matrix elements  $f_x, f_y$  and  $s_{xx}, s_{xy}, s_{yy}$  with the molecular parameters such as the transition dipole moments, the angles between these transitions and the energies of the levels.

We first consider the more general four-state, two-intermediate-level model (or two scenarios model) described in [20] and presented in Fig. 3(a). As described in [20], the tensor components may be presented as  $S_{\alpha\beta} = S_{\alpha\beta}^{(1)} + S_{\alpha\beta}^{(2)}$ , where upper indexes (1) and (2) indicate the first and the second scenarios of 2PA, and  $\alpha, \beta$  indicates to the projections in the plane ( $x, y$ ). If the first scenario involves the transitions  $S_0 \rightarrow S_1$  and  $S_1 \rightarrow S_f$  (1 is the first intermediate level and  $f$  is the final level) and the second scenario involves transitions  $S_0 \rightarrow S_n$  and  $S_n \rightarrow S_f$  ( $n$  is the second intermediate level), matrix elements  $S_{\alpha\beta}^{(1)}$  and  $S_{\alpha\beta}^{(2)}$  may be rewritten as

$$S_{\alpha\beta}^{(1)} = \frac{\mu_\alpha^{01} \mu_\beta^{1f}}{\Delta E_1} + \frac{\mu_\beta^{01} \mu_\alpha^{1f}}{\Delta E_1} \quad \text{and} \quad S_{\alpha\beta}^{(2)} = \frac{\mu_\alpha^{0n} \mu_\beta^{nf}}{\Delta E_n} + \frac{\mu_\beta^{0n} \mu_\alpha^{nf}}{\Delta E_n}, \quad (4)$$

where  $\mu_\alpha$  and  $\mu_\beta$  are the dipole moments of the participating transitions in the direction  $\alpha$  and  $\beta$ ;  $\Delta E_1 = \hbar\omega_1 - \hbar\omega$ ,  $\Delta E_n = \hbar\omega_n - \hbar\omega$  and  $\omega$  is the radiation frequency (see Fig. 3(a)). Using Eq. (4), we can write the  $xx, xy$  and  $yy$  components of  $\mathbf{S}$  as,

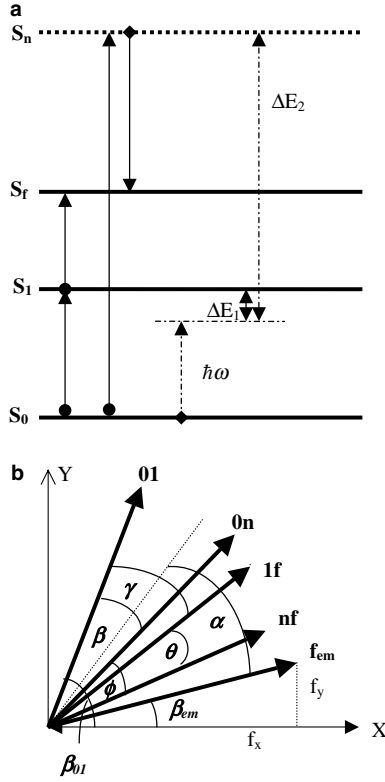


Fig. 3. Energy states  $S_0$ ,  $S_1$ ,  $S_f$  and  $S_n$  (a), and schematic diagram for four-state two-intermediate level ( $S_1$  and  $S_n$ ) model (b).

$$\begin{aligned}
 S_{xx} &= 2 \frac{\mu_x^{01} \mu_x^{1f}}{\Delta E_1} + 2 \frac{\mu_x^{0n} \mu_x^{nf}}{\Delta E_2}; \\
 S_{yy} &= 2 \frac{\mu_y^{01} \mu_y^{1f}}{\Delta E_1} + 2 \frac{\mu_y^{0n} \mu_y^{nf}}{\Delta E_2}; \\
 S_{xy} &= \frac{\mu_x^{01} \mu_y^{1f}}{\Delta E_1} + \frac{\mu_x^{0n} \mu_y^{nf}}{\Delta E_2} + \frac{\mu_y^{01} \mu_x^{1f}}{\Delta E_1} + \frac{\mu_y^{0n} \mu_x^{nf}}{\Delta E_2}.
 \end{aligned} \quad (5)$$

The next step is to find the normalized matrix elements  $s_{xx}$ ,  $s_{yy}$ ,  $s_{xy}$  using the normalization condition  $s_{\alpha\beta} = \frac{S_{\alpha\beta}}{\sqrt{\sum_{\alpha\beta} S_{\alpha\beta}^2}}$  presented in [8]. After normalization

$$\begin{aligned}
 s_{xx} &= \frac{S_{xx}}{\sqrt{S_{xx}^2 + S_{yy}^2 + 2S_{xy}^2}}, \quad s_{yy} = \frac{S_{yy}}{\sqrt{S_{xx}^2 + S_{yy}^2 + 2S_{xy}^2}} \quad \text{and} \\
 s_{xy} &= \frac{S_{xy}}{\sqrt{S_{xx}^2 + S_{yy}^2 + 2S_{xy}^2}}.
 \end{aligned} \quad (6)$$

Substituting Eq. (5) into (6), gives the normalized matrix elements  $s_{xx}$ ,  $s_{yy}$ ,  $s_{xy}$ , expressed in terms of the molecular parameters as in Eq. (3). However, Eq. (3) includes not only the normalized matrix elements of the 2PA tensor  $\mathbf{S}$  but also the normalized components of the emission dipole moment  $\mathbf{F}$ :  $f_x = \frac{F_x}{\sqrt{|\mathbf{F}|^2}}$  and  $f_y = \frac{F_y}{\sqrt{|\mathbf{F}|^2}}$  [8]. To connect these components with the absorbing dipoles, we consider the diagram shown in Fig. 3(b). It is possible to show that  $f_x = \cos(\beta_{em})$  and  $f_y = \sin(\beta_{em})$ , where  $\beta_{em} = \beta_{01} - (\frac{\gamma}{2} + \alpha)$ . The angle  $\beta_{01}$  can be written as a ratio of corresponding

$\mu_x$  and  $\mu_y$  projections and the normalized absorbing dipole  $\mu_{01}$ :  $\cos(\beta_{01}) = \frac{\mu_x^{01}}{\mu_{01}}$  and  $\sin(\beta_{01}) = \frac{\mu_y^{01}}{\mu_{01}}$ . Inserting these functions into equations for  $f_x$  and  $f_y$ , we can rewrite:

$$f_x = \frac{\mu_x^{01}}{\mu_{01}} a + \frac{\mu_y^{01}}{\mu_{01}} b \quad \text{and} \quad f_y = \frac{\mu_y^{01}}{\mu_{01}} a - \frac{\mu_x^{01}}{\mu_{01}} b, \quad (7)$$

where  $a = \cos(\frac{\gamma}{2} + \alpha)$  and  $b = \sin(\frac{\gamma}{2} + \alpha)$ . Substituting Eqs. (6) and (7) into (3), we obtain  $r_{2PA}$  in the four-state, two-intermediate level model. In the final formula,  $r_{2PA}$  should be expressed in terms of the absorbing dipoles  $\mu_{01}$ ,  $\mu_{0n}$ ,  $\mu_{1f}$ ,  $\mu_{nf}$  (not their projections), and angles  $\alpha$ ,  $\beta$ ,  $\gamma$ ,  $\theta$  between transitions and detuning energies  $\Delta E_1$ ,  $\Delta E_2$ . After algebraical transformation and taking into account that:

$$\begin{aligned}
 \mu_x^{01} \mu_y^{0n} - \mu_y^{01} \mu_x^{0n} &= -\mu_{01} \mu_{0n} \sin \beta; \\
 \mu_x^{01} \mu_x^{0n} + \mu_y^{01} \mu_y^{0n} &= \mu_{01} \mu_{0n} \cos \beta; \\
 \mu_x^{01} \mu_y^{1f} - \mu_y^{01} \mu_x^{1f} &= -\mu_{01} \mu_{1f} \sin \gamma; \\
 \mu_x^{01} \mu_x^{1f} + \mu_y^{01} \mu_y^{1f} &= \mu_{01} \mu_{1f} \cos \gamma; \\
 \mu_x^{1f} \mu_y^{nf} - \mu_y^{1f} \mu_x^{nf} &= -\mu_{1f} \mu_{nf} \sin \theta; \\
 \mu_x^{1f} \mu_x^{nf} + \mu_y^{1f} \mu_y^{nf} &= \mu_{1f} \mu_{nf} \cos \theta; \\
 \mu_x^{01} \mu_y^{nf} - \mu_y^{01} \mu_x^{nf} &= -\mu_{01} \mu_{nf} \sin(\gamma + \theta); \\
 \mu_x^{01} \mu_x^{nf} + \mu_y^{01} \mu_y^{nf} &= \mu_{01} \mu_{nf} \cos(\gamma + \theta); \\
 \mu_x^{0n} \mu_y^{1f} - \mu_y^{0n} \mu_x^{1f} &= -\mu_{0n} \mu_{1f} \sin(\gamma - \beta); \\
 \mu_x^{0n} \mu_x^{1f} + \mu_y^{0n} \mu_y^{1f} &= \mu_{0n} \mu_{1f} \cos(\gamma - \beta); \\
 \mu_x^{0n} \mu_y^{nf} - \mu_y^{0n} \mu_x^{nf} &= -\mu_{0n} \mu_{nf} \sin(\gamma + \theta - \beta); \\
 \mu_x^{0n} \mu_x^{nf} + \mu_y^{0n} \mu_y^{nf} &= \mu_{0n} \mu_{nf} \cos(\gamma + \theta - \beta),
 \end{aligned}$$

we finally obtain the expression:

$$r_{2PA} = \frac{18(K_1 + K_2)K_3 - 8K_3^2 + K_4}{7(K_3^2 + K_4)}, \quad (8)$$

where

$$\begin{aligned}
 K_1 &= \Delta E_2 \mu_{01} \mu_{1f} \cos(\frac{\gamma}{2} + \alpha) \cos(\frac{\gamma}{2} - \alpha); \\
 K_2 &= \Delta E_1 \mu_{0n} \mu_{nf} \cos(\frac{\gamma}{2} - \alpha + \theta) \cos(\frac{\gamma}{2} + \alpha - \beta); \\
 K_3 &= \Delta E_2 \mu_{01} \mu_{1f} \cos \gamma + \Delta E_1 \mu_{0n} \mu_{nf} \cos(\gamma + \theta - \beta); \\
 K_4 &= \Delta E_1^2 \mu_{0n}^2 \mu_{nf}^2 [1 + \cos^2(\gamma + \theta - \beta)] \\
 &\quad + \Delta E_2^2 \mu_{01}^2 \mu_{1f}^2 (1 + \cos^2 \gamma) + 2 \Delta E_1 \Delta E_2 \mu_{01} \mu_{0n} \mu_{1f} \mu_{nf} \\
 &\quad \times [\cos(\gamma + \theta) \cos(\gamma - \beta) + \cos \theta \cos \beta].
 \end{aligned}$$

The three-state model is the simplest model for 2PA with absorbing transition dipoles  $S_0 \rightarrow S_1$  and  $S_1 \rightarrow S_f$  (1 is the only intermediate level and f is the final level). In this case,  $\mu_{0n} = \mu_{nf} = 0$ ;  $\beta = \theta = 0$ ;  $\Delta E_1 = \Delta E_2 = \Delta E$ , and Eq. (8) can be simplified to

$$r_{2PA} = \frac{18 \cos(\frac{\gamma}{2} - \alpha) \cos(\frac{\gamma}{2} + \alpha) \cos \gamma - 7 \cos^2 \gamma + 1}{7(2 \cos^2 \gamma + 1)}. \quad (9)$$

The main difference between Eqs. (8) and (9) is that in the three-state model,  $r_{2PA}$  depends on only two angles:  $\gamma$  (between  $\mu_{01}$  and  $\mu_{1f}$ ) and  $\alpha$  (between the bisecting line of the

angle  $\gamma$  and the emission dipole, and does not depend on the values of the absorbing dipole moments or the detuning energy. We note that Eq. (9) can be transformed into the equation presented in [21] for the degree of polarization. If the absorbing dipoles are parallel,  $\gamma = 0$  and  $\alpha$  becomes equal to the angle between the absorbing and emitting dipoles. Then  $r_{2PA}$  reduces to the well-known formula [16]:

$$r_{2PA} = \frac{6\cos^2\alpha - 2}{7}, \quad (10)$$

In the case of  $\alpha = 0^\circ$ ,  $r_{2PA}$  reaches its maximum value  $r_{2PA}^{\max} = 0.57$ . If  $\alpha = 90^\circ$ , the anisotropy value reaches its largest negative value:  $r_{2PA}^{\min} = -0.29$ . In contrast to  $r_{1PA}$ , the two-photon anisotropy depends on the mutual orientation of three dipole moments participating in 2PA and corresponding to the transitions:  $S_0 \rightarrow S_1$ ,  $S_1 \rightarrow S_f$  and  $S_1 \rightarrow S_0$ . A general diagram of the 2D-space orientation for these dipoles is presented in Fig. 4. Angle  $\alpha_{em} = \alpha + \frac{\gamma}{2}$ , between the absorption  $S_0 \rightarrow S_1$  and the emission  $S_1 \rightarrow S_0$  dipole moments, can be found from one-photon anisotropy measurements. The two-photon anisotropy,  $r_{2PA}$ , as a func-

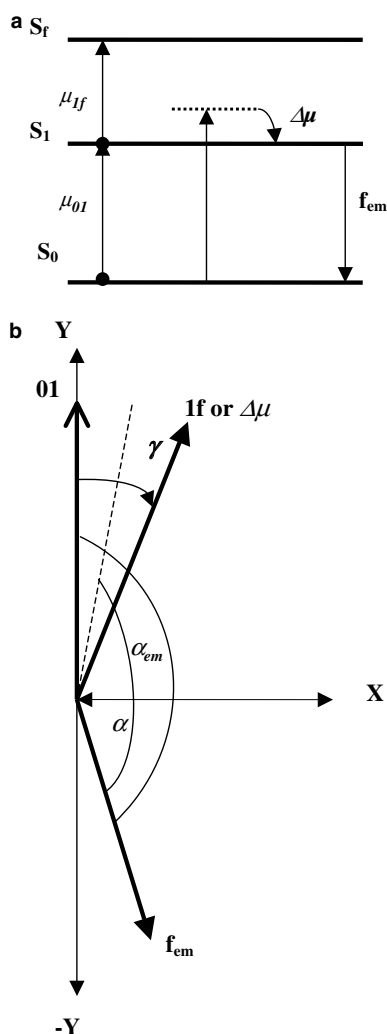


Fig. 4. Energy states  $S_0$ ,  $S_1$  and  $S_f$  (a), and schematic diagram for three-state one-intermediate level ( $S_1$ ) model (b).

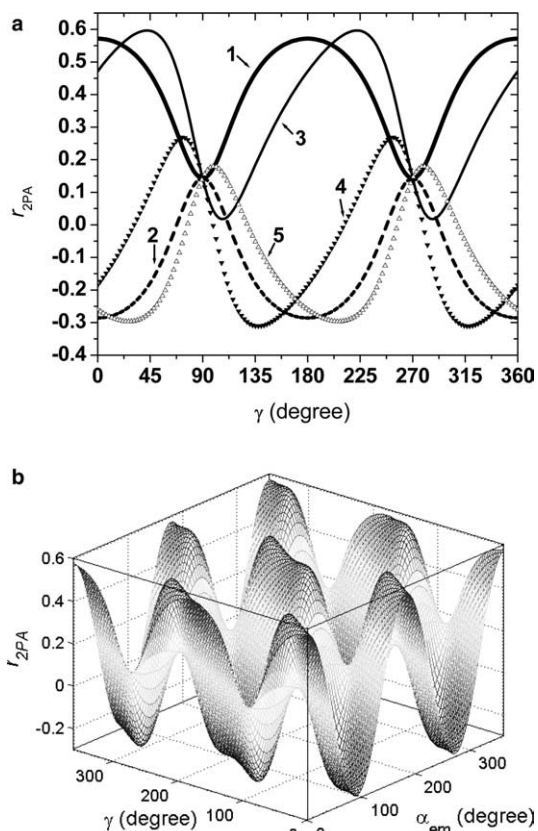


Fig. 5. (a) Two-photon anisotropy  $r_{2PA}$ , calculated in three-state model, as function of the angle  $\gamma$  between two absorbing dipoles at:  $\alpha_{em} = 0^\circ$  (1);  $90^\circ$  (dashed curve 2);  $20^\circ$  (3);  $70^\circ$  (4), and  $100^\circ$  (5). (b) 3D picture of  $r_{2PA}$ , calculated in three-state model, as function of  $\gamma$  and  $\alpha_{em}$ .

tion of angle  $\gamma$  between two absorbing dipoles is shown in Fig. 5. It is seen that  $r_{2PA}$  is a complicated function of  $\gamma$ . At  $\gamma = 0^\circ$  or  $360^\circ$  the anisotropy  $r_{2PA}$  changes from its maximum value 0.57 (at  $\alpha_{em} = 0^\circ$  or  $180^\circ$ ;  $180^\circ$  period) to its largest negative value  $-0.29$  (at  $\alpha_{em} = 90^\circ$  or  $270^\circ$ ). At  $\gamma = 90^\circ$  and  $270^\circ$  all curves converge to a point  $r_{2PA} = 0.14$ . As can be seen from this figure, the highest anisotropy value  $r_{2PA} \approx 0.6$  corresponds to  $\gamma \approx 42^\circ$  and  $222^\circ$  ( $180^\circ$  period) at  $\alpha_{em} = 20^\circ$  or  $200^\circ$ , and the smallest anisotropy value  $r_{2PA} \approx -0.3$  corresponds to  $\gamma \approx 27^\circ$  and  $207^\circ$  at  $\alpha_{em} = 100^\circ$  or  $280^\circ$ .

#### 4. Molecular modeling for polymethine and fluorene molecules

##### 4.1. Analysis of two-photon anisotropy using a three-state model

Let us consider the most typical case for the polymethine dyes. It is commonly known that for many PDs the angle between the absorbing  $S_0 \rightarrow S_1$  and emitting  $S_1 \rightarrow S_0$  dipoles is small:  $\alpha_{em} = \alpha + \frac{\gamma}{2} \leq 20^\circ$ . This conclusion follows from high one-photon anisotropy values 0.35–0.38 within the first absorption band [1,22]. Taking into account the schematic diagram presented in Fig. 4, we consider the

orientation of the emission dipole ranging from parallel to the  $S_0 \rightarrow S_1$  transition orientation, that is  $\alpha_{em} = 0$  (or anti-parallel,  $\alpha_{em} = 180^\circ$ , which is the same) to  $20^\circ$ . A set of curves for  $r_{2PA}$  as a function of  $\gamma$  ranging from  $0^\circ$  to  $20^\circ$  at several  $\alpha_{em}$  is shown in Fig. 6. It is seen that  $r_{2PA}$  changes from its maximum value  $\approx 0.6$  at  $\gamma = 42^\circ$  ( $\alpha_{em} = 20^\circ$ ) to its lowest value  $\approx 0.018$  at  $\gamma = 107^\circ$  at the same  $\alpha_{em}$ . As was mentioned above, at  $\gamma = 90^\circ$  all curves converge to a point  $r_{2PA} = 0.14$  independently of  $\alpha_{em}$ .

It is commonly accepted that two-photon excitation to the first excited state  $S_1$  involves the two dipole moments:  $\mu_{01}$  and  $\Delta\mu$  (vector difference between permanent  $S_0$  and  $S_1$  dipoles), where the  $S_1$  state is the intermediate state. Two-photon excitation to the second excited state  $S_2$  involves  $\mu_{01}$  and  $\mu_{12}$  at the same  $S_1$  intermediate state. According to the traditional quantum-chemical theories [23], for all symmetrical polymethine dyes  $\Delta\mu$  is oriented perpendicular to  $\mu_{01}$ , and transition dipoles  $\mu_{01}$  and  $\mu_{12}$  are oriented parallel (or anti-parallel). The near parallel orientation of  $\mu_{01}$  and  $\mu_{12}$  for several PDs was confirmed by us experimentally [1]. Applying this approach to Fig. 6, we can come to the conclusion that for 2PA to  $S_1$  ( $\gamma = 90^\circ$ ),  $r_{2PA} = 0.14$  for all orientations of the emission dipole, and for 2PA to  $S_2$  ( $\gamma = 0^\circ$  or  $180^\circ$ ),  $r_{2PA}$  values are in the range from 0.47 ( $\alpha_{em} = 20^\circ$ ) to 0.57 ( $\alpha_{em} = 0^\circ$ ).

The next step is to compare these theoretical dependences with the experimental results. The measurements of two-photon anisotropy have been performed by us for several symmetrical and asymmetrical PDs and fluorenes (structures shown in Fig. 1). For these molecules, experimental  $r_{2PA}$  values range from 0.47 to 0.57 and remain almost constant over several electronic transitions. Experimental data for  $r_{1PA}$  and  $r_{2PA}$  are presented in Figs. 7 and 8. As can be seen from Fig. 7, for the symmetrical PDs 2350 and 3428,  $r_{2PA} \approx 0.47$ – $0.49$  over a broad spectral range, which covers at least two electronic transitions  $S_0 \rightarrow S_1$  and  $S_0 \rightarrow S_2$ . At the same time,  $r_{1PA}^{max} \approx 0.38$  indicating that  $\alpha_{em}$  does not exceed  $10^\circ$ . As seen in Fig. 6, the theoretical values of  $r_{2PA}$  are equal to  $\approx 0.55$  for 2PA to the  $S_2$  state ( $\gamma = 0^\circ$ ) and 0.14 for 2PA to the  $S_1$  state ( $\gamma = 90^\circ$ ). Both excitation cases contradict the experimental

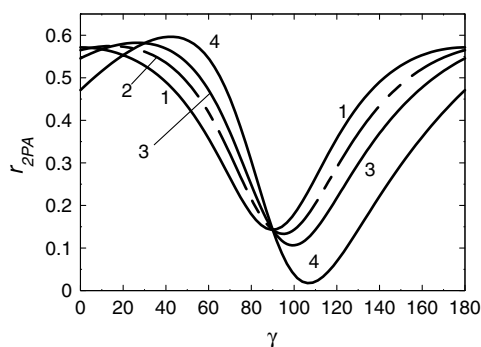


Fig. 6. Two-photon anisotropy  $r_{2PA}$  as function of the angle  $\gamma$  between two absorbing dipoles at  $\alpha_{em} = 0^\circ$  (1);  $5^\circ$  (dashed curve 2);  $10^\circ$  (3), and  $20^\circ$  (4).

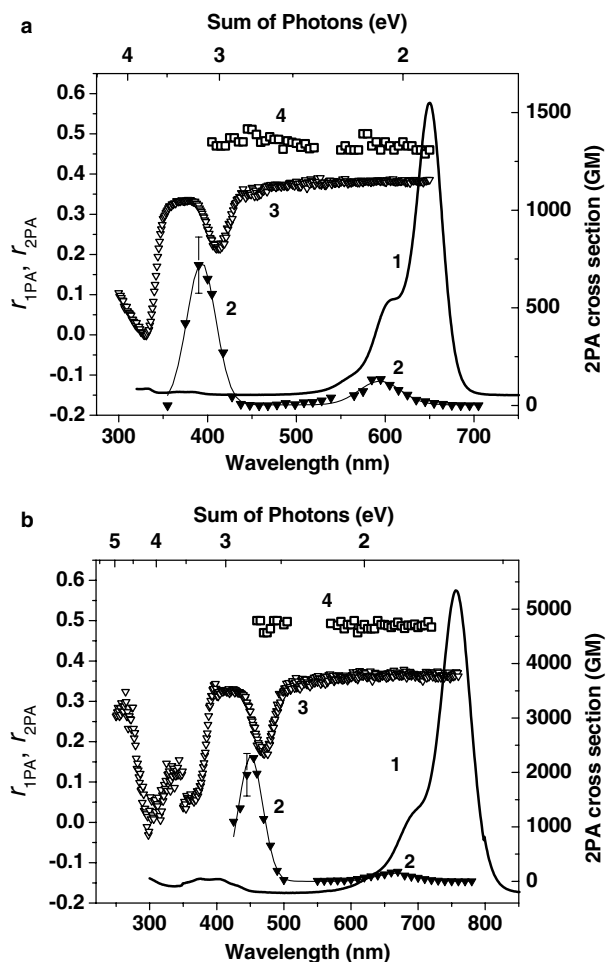


Fig. 7. Linear absorption (1) and 2PA (2) in ethanol; one-photon anisotropy (3) and two-photon anisotropy (4) spectra in glycerol for PD 2350 (a) and PD 3428 (b). For comparison with linear absorption, two-photon absorption and two-photon anisotropy spectra are presented as functions of  $\lambda_{pump}/2$ . Uncertainties:  $r_{1PA}$ :  $\pm 5\%$ ,  $r_{2PA}$ :  $\pm 10\%$ , 2PA cross-section:  $\pm 20\%$ .

results. Thus, for symmetrical PDs, the three-state model cannot adequately model two-photon excitation to either  $S_1$  or  $S_2$ . For the symmetrical fluorene dye 2 (see Fig. 8c), we measure  $r_{2PA} \approx 0.53$  for both states, which is close to the theoretical value for  $S_2$  but disagrees with the theoretical result for the  $S_1$  state. For symmetrical molecules, 2PA into the highly allowed one-photon absorption band  $S_0 \rightarrow S_1$  is forbidden by dipole selection rules. However, vibronic coupling breaks the symmetry and thus the dipole selection rules, resulting in a weakly allowed 2PA band at the vibronic shoulder of the  $S_0 \rightarrow S_1$  band [24]. This is revealed by the high sensitivity of the up-converted fluorescence method. Because the vibronic coupling causes  $\gamma$  to deviate from  $90^\circ$ , the theoretically predicted  $r_{2PA} = 0.14$  is not observed.

Now we apply the three-state model for the asymmetrical molecules Styryl 1, PD 2665 and fluorene dye 1. Experimental results are shown in Fig. 8(a)–(c). Quantum-chemical calculations performed for these molecules, show that  $\mu_{01}$

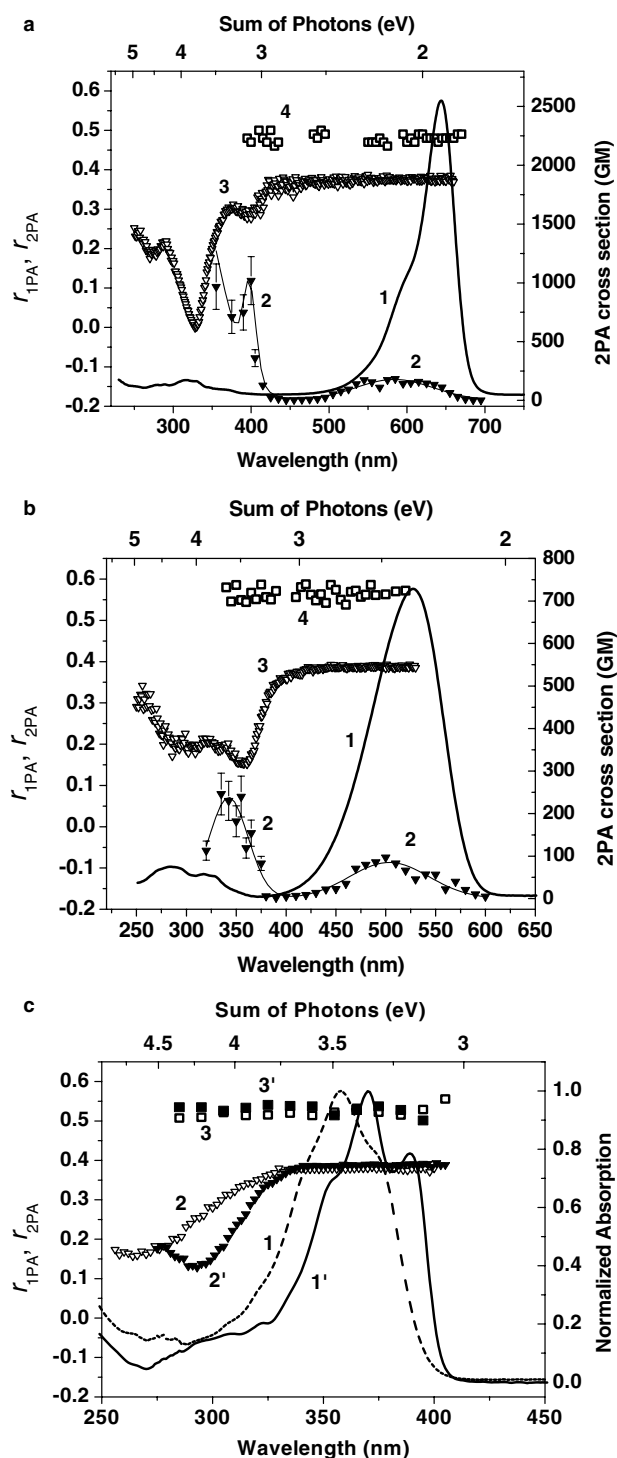


Fig. 8. Linear absorption (1) and 2PA spectra (2) in ethanol; one-photon anisotropy (3) and two-photon anisotropy (4) in glycerol for PD 2665 (a) and Styryl 1 (b). (c) Linear absorption (1,1'), one-photon anisotropy (2,2') and two-photon anisotropy (3,3') in *p*-THF for fluorene 1 (1, 2, 3) and fluorene 2 (1', 2', 3'). For comparison with linear absorption, two-photon absorption and two-photon anisotropy spectra are presented as functions of  $\lambda_{\text{pump}}/2$ . Uncertainties:  $r_{1\text{PA}}$ :  $\pm 5\%$ ,  $r_{2\text{PA}}$ :  $\pm 10\%$ , 2PA cross-section:  $\pm 20\%$ .

and  $\mu_{12}$  are oriented almost parallel (angles are within  $5^\circ$ ) similar to the symmetrical molecules. However,  $\Delta\mu$  shows a large deviation from an orientation perpendicular to

$\mu_{01}$ . These angles  $\gamma$  for Styryl 1, PD 2665 and fluorene 1 equal  $26^\circ$ ,  $43^\circ$  and  $37^\circ$ , respectively. Substituting these  $\gamma$ 's into Eq. (9), as well as using the experimental value of  $\alpha_{\text{em}} = 10^\circ$ , which is the same for all these molecules, we calculated that  $r_{2\text{PA}} \approx 0.55$ – $0.56$  for two-photon transitions to  $S_1$  and  $S_2$  states. Thus, the three-state model can be used to model the asymmetrical molecules but is inadequate to model the symmetrical ones.

#### 4.2. Analysis of two-photon anisotropy using the four-state model

In this section we apply the more complicated four-state, two-intermediate-level model for the analysis of two-photon anisotropy for the symmetrical molecules. According to Eq. (8),  $r_{2\text{PA}}$  becomes a function of the mutual orientation in 2D-space of all 5 dipoles participated in the 2PA process ( $\mu_{01}$ ,  $\mu_{1E}$ ,  $\mu_{0n}$ ,  $\mu_{nE}$  and emission dipole  $\mu_{10}$ ).  $r_{2\text{PA}}$  also depends on the values of the four dipoles moments and two detuning energies. Most of these 10 molecular parameters can be found experimentally from one-photon anisotropy spectra and can be calculated quantum-chemically. Here, we consider separately the case of two-photon excitation to  $S_1$  and to the higher excited-state  $S_2$ .

Firstly, we analyze the case of two-photon excitation of symmetrical molecules to state  $S_2$  considering the following two simultaneous scenarios or channels:  $S_0 \rightarrow S_1$  and  $S_1 \rightarrow S_2$  (first) and  $S_0 \rightarrow S_4$  and  $S_4 \rightarrow S_2$  (second). The choice of  $S_4$  as the second intermediate state for PDs is connected with our observation, taken from one-photon anisotropy spectra, that the angle  $\beta$  (between two scenarios or between  $\mu_{01}$  and  $\mu_{04}$ ) is typically one of the largest angles ( $\approx 60^\circ$ ) among the measurable  $S_0 \rightarrow S_n$  transitions. We show below (in Fig. 11(a)) that an increase of the angle  $\beta$  can lead to a decrease of  $r_{2\text{PA}}$ , which becomes closer to the experimental values. In fact, from the theoretical analysis, any  $S_n$  state with sufficiently large angle  $\beta$  between the  $\mu_{01}$  and  $\mu_{0n}$  can play the role of the second intermediate state in order to get closer to the experimental value. According to traditional quantum-chemical theories, the transitions within each scenario can be anti-parallel ( $\gamma = \phi = 180^\circ$ ) or parallel ( $\gamma = \phi = 0^\circ$ ) to each other, where  $\gamma$  is an angle inside of the first scenario and  $\phi$  is the angle inside of the second scenario [23]. Therefore, we start our analysis from this classical case schematically presented in Fig. 9(a). The dependence of  $r_{2\text{PA}}$  on angle  $\gamma$  for PD 2350, calculated by Eq. (8), is shown in Fig. 10, curve 1. Typically, for polymethines, the contribution of the second channel is small:  $\mu_{04}\mu_{42} \ll \mu_{01}\mu_{12}$ , therefore, curve 1 corresponds to the three-state model and completely overlaps with curve 2 in Fig. 6. In this case,  $r_{2\text{PA}}$  depends only on  $\gamma$  and  $\alpha_{\text{em}}$  and does not change significantly with changes of  $\beta$  and  $\phi$  ( $\phi = \theta + \gamma - \beta$ ), which is shown in the 3D plot in Fig. 10(b). Theoretically there is a way to decrease  $r_{2\text{PA}}$  closer to experimental values keeping the parallel or anti-parallel orientation of transitions inside each channel. For this purpose we consider an increase in the contribu-

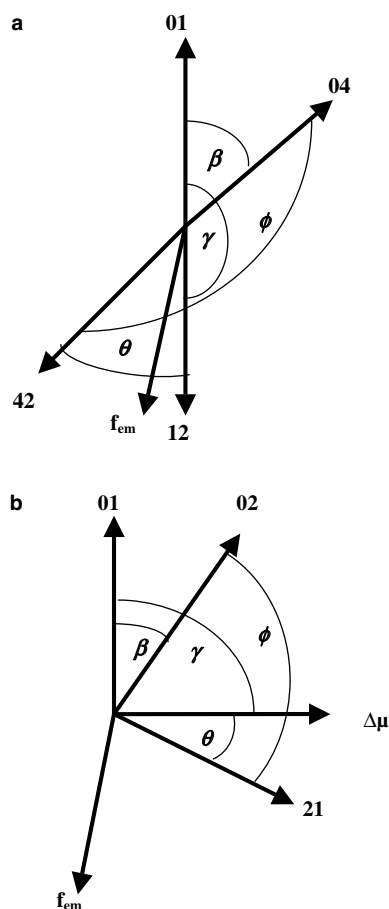


Fig. 9. Schematic diagram for four-state two-intermediate level model at two-photon excitation to  $S_2$  (a) and  $S_1$  (b).

tion of the second channel. Fig. 10(a) (curves 2 and 3) demonstrates these results for the case  $\mu_{04}\mu_{42} \geq \mu_{01}\mu_{12}$ . The 3D plots of  $r_{2PA}$ , calculated in four-state model, as functions of  $\beta$ ,  $\gamma$  (a) and  $\beta$ ,  $\phi$  (b) at an increased contribution of the second channel, are presented in Fig. 11(a) and (b). For the polymethine molecules, this case may be achieved by considering the second channel as a superposition of all possible channels oriented at relatively large angles to the first excitation channel. It is important to note that in contrast to PDs, some molecules from the other classes of organic compounds are characterized by strong transitions to the second or higher excited-states with dipole moments comparable to  $\mu_{01}$ . For example, the symmetrical 9,9-didecyl-2,7-bis-(*N,N*-diphenylamino)fluorene, reported in [11], shows relatively large transition dipole moments (up to 6 D) to the higher excited-states at  $\mu_{01} = 8$  D. Its molecular parameters, revealed from quantum-chemical calculations and substituted into Eq. (8), give  $r_{2PA} \approx 0.27$  which is close to its experimental value [11]. This confirms that the four-state, two-intermediate-level model can be used for the explanation of  $r_{2PA}$  into  $S_2$  state, if the contribution of the effective second channel is comparable with the contribution of the first one.

Secondly, we analyze the case of two-photon excitation of symmetrical molecules into the  $S_1$  state, which is not al-

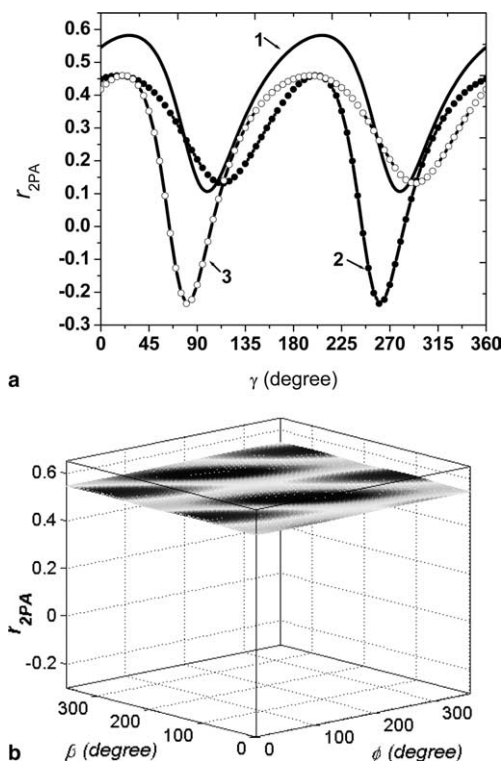


Fig. 10. (a) Two-photon anisotropy  $r_{2PA}$ , calculated in four-state model, as function of  $\gamma$ . Curve 1:  $\alpha_{em} = 10^\circ$ ;  $\mu_{01} = 13.5$  D;  $\mu_{12} = \mu_{04} = \mu_{42} = 1$  D;  $\beta = 60^\circ$ ;  $\phi$  is an angle between dipoles inside of the second channel,  $\phi = 0^\circ$  (or  $180^\circ$ );  $\Delta E_1 = 0.5$  eV;  $\Delta E_2 = 2.5$  eV. This curve coincides with curve 3 from Fig. 6 obtained from three-state model. Curves 2 and 3:  $\alpha_{em} = 10^\circ$ ;  $\mu_{01} = 13.5$  D;  $\mu_{12} = 1$  D;  $\mu_{04} = \mu_{42} = 6$  D;  $\beta = 60^\circ$ ;  $\Delta E_1 = 0.5$  eV;  $\Delta E_2 = 2.5$  eV;  $\phi = 0^\circ$  (for curve 2) and  $\phi = 180^\circ$  (for curve 3). (b) 3D picture of  $r_{2PA}$ , calculated in four-state model, as function of  $\beta$  and  $\phi$ .

lowed by symmetry rules. We consider the two following simultaneous channels of excitation: the first channel, involving  $\mu_{01}$  and  $\Delta\mu$ , and the second channel, involving  $\mu_{02}$  and  $\mu_{21}$  (see Fig. 9(b)). According to the traditional quantum-chemical theories, the transitions inside of each scenario are perpendicular to each other ( $\gamma = \phi = 90^\circ$ ) [23]. Therefore, in this classical case,  $r_{2PA} = 0.14$ , independently of other molecular parameters, and can be increased in only one way, i.e., by allowing the deviation of angles  $\gamma$  or  $\phi$  (or both) from  $90^\circ$ . In contrast to the previous case of two-photon excitation to  $S_2$ , an increase in the contribution of the second channel cannot change  $r_{2PA}$ .

As was mentioned above, for the symmetrical molecules 2PA into  $S_1$  is forbidden. A blue-shifted and weakly allowed 2PA band can be revealed within the linear  $S_0 \rightarrow S_1$  absorption due to vibronic coupling [24]. Our understanding is that this vibronic coupling can change the angle between the  $\mu_{01}$  and  $\Delta\mu$ , leading to the ground-state symmetry breaking in the charge distribution. Applying experimental values of  $r_{2PA}$  to Eq. (8), for the case of the contribution of the second channel is comparable to that of the first, or to Eq. (9), for the case of the contribution of the second channel is much smaller, we find values of  $\gamma$ . Calculations shows that for PD 2350  $\gamma \approx 55^\circ$  (deviation from the perpendicular orientation equals  $35^\circ$ ). Thus, we propose that two-photon

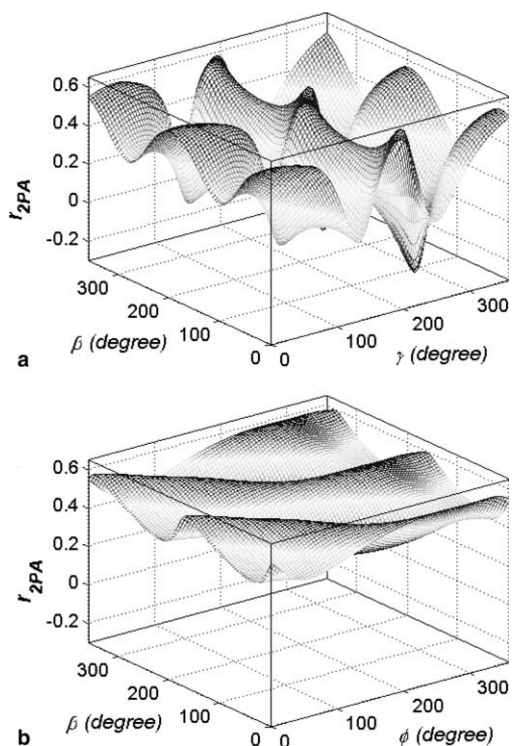


Fig. 11. 3D pictures of  $r_{2PA}$ , calculated in four-state model, as functions of  $\beta$ ,  $\gamma$  (a) and  $\beta$ ,  $\phi$  (b). Molecular parameters for calculations:  $\alpha_{em} = 10^\circ$ ;  $\mu_{01} = 13.5$  D;  $\mu_{12} = 1$  D;  $\mu_{04} = \mu_{42} = 6$  D;  $\Delta E_1 = 0.5$  eV;  $\Delta E_2 = 2.5$  eV;  $\phi = 180^\circ$  (a);  $\gamma = 180^\circ$  (b).

anisotropy can serve as a useful tool for estimation of the ground-state symmetry breaking.

#### 4.3. Symmetry breaking in symmetrical polymethine dyes

We recently reported the linear and non-linear properties of symmetrical PDs with a long conjugated chromophore both experimentally and theoretically [25], see also references therein. We proposed that the charge distribution in the ground state can be presented as a mixture of two forms with symmetrical and asymmetrical charge distributions and corresponding bond length alternations. Unusual spectral properties of these molecules (broad absorption bands and strong dependence on solvent polarity) were explained by involving the concept of solitons, or mobile defects, in the charged conjugated systems [26]. PD molecules with shorter chains are characterized by much narrower absorption bands which are almost solvent independent. Therefore, it is logical to assume that for these molecules, contribution of an asymmetrically charged form is much smaller than for PDs having a long chain, and a symmetrical charge form dominates. However, even a small contribution of an asymmetrical form can lead to non-equality in the charge transfer from the terminal groups to the chain center affecting the orientation of the transition moments. Note that this effect cannot essentially change the orientation of the large  $S_0 \rightarrow S_1$  transition dipole moment since for both forms charge transfer occurs

in the direction of the chromophore. However, for other transition dipoles, which are at least one order of magnitude smaller, the difference in the charge transfer from the terminal groups to the center of the chain can strongly affect their orientations. An especially strong effect can be observed for the “perpendicular” (to  $S_0 \rightarrow S_1$ ) transitions, such as  $\Delta\mu$ ,  $S_0 \rightarrow S_2$ ,  $S_0 \rightarrow S_4$ . Possible deviations of transition moments from the “classical” directions induced by the contribution of the asymmetrical form are schematically shown in Fig. 12. It is seen that the asymmetrical charge transfer from the terminal groups can change the direction of  $\mu_{02}$  relative to  $\mu_{01}$ . However, we cannot predict how the deviation of  $\mu_{02}$  will change the “classical” orientation of  $\mu_{12}$  (parallel or anti-parallel to  $\mu_{01}$ ). Further development of quantum-chemical theory is necessary. The assumption about the ground-state symmetry breaking, affecting the orientations of higher excited-state transitions relative to  $\mu_{01}$ , can explain why in one-photon anisotropy measurements the “classical” minimal anisotropy value  $r_{1PA} = -0.2$ , corresponding to an angle  $\alpha_{em} = 90^\circ$ , has not been observed. The maximum angles observed experimentally for the “perpendicular” transitions in PDs were  $60^\circ$ – $65^\circ$ .

Finally, we have performed a modeling of the spectral dependence of  $r_{2PA}$  for symmetrical PD 2350 using the four-state, two-intermediate-level model. The results are shown in Fig. 13. As can be seen,  $r_{2PA} \approx \text{const}$  within the first and second absorption bands, if we allow the deviations of the participating dipoles to be  $\approx 35^\circ$  for  $\Delta\mu$  (from the perpendicular “classical” orientation), and  $\approx 17^\circ$  for  $\mu_{12}$  (from the anti-parallel “classical” orientation). As was discussed in Section 4.1, quantum-chemical calculations performed for asymmetrical molecules have shown a large deviation of  $\Delta\mu$  from being perpendicular to  $\mu_{01}$  (even for the weakly asymmetrical PD 2665). The resulting orientation angles  $\gamma$  are from  $26^\circ$  to  $43^\circ$ . Therefore, as can

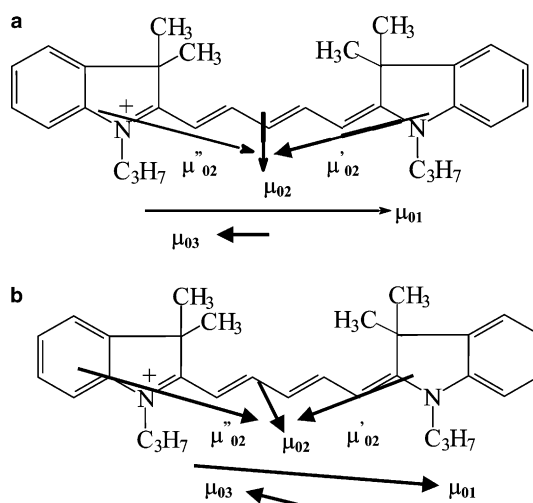


Fig. 12. Schematic presentation of orientation of the transition dipole moments for symmetrical (a) and asymmetrical (b) forms.  $\mu''_{02}$  and  $\mu'_{02}$  indicate a partial charge transfer from each terminal group to polymethine chromophore.

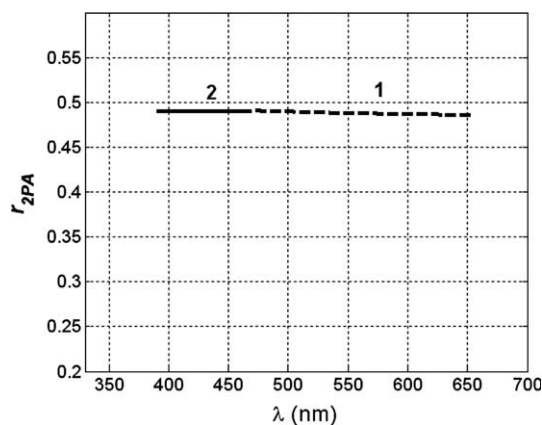


Fig. 13. Calculated dependence of  $r_{2PA}$  at 2PA to  $S_1$  state (1) and 2PA to  $S_2$  state (2) based on four-state model. Molecular parameters for (1) are:  $\alpha_{em} = 10^\circ$ ;  $\mu_{01} = 13.5$  D;  $\Delta\mu = 0.6$ ;  $\mu_{02} = 1.2$  D;  $\mu_{21} = 1$  D;  $\phi = 90^\circ$ ;  $\beta = 32^\circ$ ;  $\gamma = 55^\circ$ . Molecular parameters for (2) are:  $\alpha_{em} = 10^\circ$ ;  $\mu_{01} = 13.5$  D;  $\mu_{12} = 1$  D;  $\mu_{04} = \mu_{42} = 1$  D;  $x = 180^\circ$ ;  $\beta = 60^\circ$ ;  $\gamma = 163^\circ$ .

be seen from Fig. 6, curve 3, at  $\gamma \approx 0^\circ$ – $50^\circ$ ,  $r_{2PA} \approx 0.5$ – $0.55$ . At the same time,  $\mu_{01}$  and  $\mu_{12}$  are still oriented almost parallel (angles  $\gamma$  are  $\leq 5^\circ$ ), similar to the symmetrical molecules, thus showing approximately the same  $r_{2PA}$  values. Therefore, we can conclude that the higher values of  $r_{2PA}$  correspond to the case of a smaller deviation of the angles from the “classical” orientation for two-photon excitation to the  $S_2$  state and a larger deviation for the excitation to the  $S_1$  state. Our understanding is that the symmetry breaking mechanism leading to an asymmetrical ground-state charge distribution, which already exists in asymmetrical molecules, is responsible for the nearly constant values of  $r_{2PA}$  for the symmetrical molecules. This effect also strongly changes the orientation of  $\Delta\mu$  and allows weak 2PA to the  $S_1$  state. To fully understand why  $r_{2PA}$  is nearly wavelength invariant will require additional experimental and theoretical studies.

## 5. Conclusions

We have described a detailed investigation of one- and two-photon anisotropy in a series of symmetrical and asymmetrical polymethine and fluorene molecules. For all the molecules discussed in this paper, experimental  $r_{2PA}$  values range from 0.47 to 0.57 and remain almost constant over several electronic transitions in spite of their one-photon anisotropy,  $r_{1PA}$ , showing a broad range of values from  $\approx 0$  to 0.38. From one-photon anisotropy studies we found the positions of electronic transitions to the higher excited-state, and calculated the angles between  $S_0 \rightarrow S_n$  ( $n = 1, 2, 3, 4$ ) transition dipoles and the emission  $S_1 \rightarrow S_0$  dipole moment. From quantum-chemical calculations we found the values of the transition dipoles moments participating in 2PA, as well as the angles between them. This knowledge was applied to perform molecular modeling and provide a deeper understand of the nature of 2PA processes in these molecules.

Based on two theoretical approaches made by Callis, [8] and Cronstrand et al. [20], we derived an expression for the two-photon anisotropy in the general four-state, two-intermediate-level model taking into account the influence of the additional second excitation channel. A simplified formula for the three-state, single-intermediate level model was also derived. A complete analysis of two-photon anisotropy using three- and four-state models allowed us to make the following conclusions.

1. The three-state model, involving dipole moments  $\mu_{01}$  and  $\Delta\mu$  (for 2PA to  $S_1$ ) and  $\mu_{01}$  and  $\mu_{12}$  (for 2PA to  $S_2$ ) at one intermediate state  $S_1$ , can be successfully applied to explain the 2PA processes in asymmetrical PDs and fluorenes with a dominant  $S_0 \rightarrow S_1$  transition. However, this model cannot be used for all the symmetrical molecules or for asymmetrical molecules with large transition dipole moments to higher excited-states comparable to  $\mu_{01}$ .
2. The four-state model was considered for the symmetrical molecules for the cases of 2PA to the higher excited-state  $S_2$  and, separately, to  $S_1$ . In the case of two-photon excitation to  $S_2$ , the two following simultaneous channels were considered: first,  $S_0 \rightarrow S_1$  and  $S_1 \rightarrow S_2$ , and second,  $S_0 \rightarrow S_n$  and  $S_n \rightarrow S_2$ . For theoretical analysis, any  $S_n$  state with sufficiently large angle  $\beta$  between  $\mu_{01}$  and  $\mu_{0n}$  dipoles can play the role of the second intermediate state. For comparison of experimental and theoretical values of  $r_{2PA}$  for polymethines, the  $S_4$  state was chosen as the second intermediate state. It is known that for PDs, the contribution of the second channel is typically small in contrast to some fluorenes which have large transition dipole moments to the higher excited-states. It was shown that experimental values of  $r_{2PA}$  for these fluorene molecules can be explained in the frame of four-state model.
3. In the case of two-photon excitation of symmetrical molecules to the  $S_1$  state, the two following simultaneous channels of excitation were considered: first, involving  $\mu_{01}$  and  $\Delta\mu$ ; and second, involving transition dipole moments  $\mu_{01}$  and  $\mu_{12}$ . Theoretical analysis shown that in this case the high  $r_{2PA}$  values can only be explained by taking into account the effect of vibronic coupling within the forbidden by symmetry rules  $S_0 \rightarrow S_1$  band. Our understanding is that this vibronic coupling can change the angle between  $\mu_{01}$  and  $\Delta\mu$  leading to ground-state symmetry breaking. This symmetry breaking phenomenon can also affect 2PA into the  $S_2$  state. Thus, experimental values of  $r_{2PA}$  for symmetrical polymethines and fluorenes with a dominant  $S_0 \rightarrow S_1$  transition can be explained by deviations of the participating transition dipole moments from the “classical” parallel and perpendicular orientations.
4. Based on the previously investigated symmetry breaking phenomenon for PDs having a long polymethine chromophore, we proposed that for PD molecules with a shorter chain even a small contribution of the form with

an asymmetrical charge distribution can lead to a non-equality in the charge transfer from the terminal groups to the chain center affecting the orientation of the transition moments. We have shown that this effect cannot essentially change the orientation of the large  $S_0 \rightarrow S_1$  transition dipole, but it strongly affects the orientations of smaller transition dipole moments (especially for the “perpendicular” transitions) such as  $\mu_{02}$ ,  $\mu_{04}$ , and the orientation of  $\Delta\mu$ . Our understanding is that, similar to the case of initially asymmetrical molecules, the ground-state symmetry breaking mechanism is also responsible for the nearly constant values of  $r_{2PA}$  for symmetrical molecules due to its strong influence on the orientation of  $\Delta\mu$ .

### Acknowledgments

We gratefully acknowledge the support of the National Science Foundation ECS 0217932, the US Army Research Laboratory, and the Naval Air Warfare Center Joint Service Agile Program (contract number N00421-04-20001). O.V.P. and M.V.B. appreciate the partial support from the Civilian Research and Development Foundation (UK-C2-2574-MO-04). L.A.P. thanks the Brazilian agency CAPES for the financial support.

### References

- [1] R.S. Lepkowitz, O.V. Przhonska, J.M. Hales, D.J. Hagan, E.W. Van Stryland, M.V. Bondar, Yu.L. Slominsky, A.D. Kachkovski, *Chem. Phys.* 286 (2003) 277.
- [2] J.M. Hales, D.J. Hagan, E.W. Van Stryland, K.J. Schafer, A.R. Morales, K.D. Belfield, P. Pacher, O. Kwon, E. Zojer, J.L. Bredas, *J. Chem. Phys.* 121 (2004) 3152.
- [3] M. Albota, D. Beljonne, J.L. Bredas, J.E. Ehrlich, J.-Y. Fu, A.A. Heikal, S. Hess, T. Kojej, M.D. Levin, S.R. Marder, D. McCord-Maughon, J.W. Perry, H. Rockel, M. Rumi, G. Subramaniam, W.W. Webb, X.-L. Wu, C. Xu, *Science* 281 (1998) 1653.
- [4] T. Kojej, D. Beljonne, F. Meyers, J.W. Perry, S.R. Marder, J.L. Bredas, *Chem. Phys. Lett.* 298 (1998) 1.
- [5] M. Rumi, J.E. Ehrlich, A.A. Heikal, J.W. Perry, S. Barlow, Z. Hu, D. McCord-Maughon, T.C. Parker, H. Rocker, S. Thayumanavan, S.R. Marder, D. Beljonne, J.L. Bredas, *J. Am. Chem. Soc.* 122 (2000) 9500.
- [6] G.S. He, T.-C. Lin, J. Dai, P.N. Prasad, R. Kannan, A.G. Dombroskie, R.A. Vaia, L.-S. Tan, *J. Chem. Phys.* 120 (2004) 5275.
- [7] C.-K. Wang, P. Macak, Yi Luo, H. Agren, *J. Chem. Phys.* 114 (2001) 9813.
- [8] P.R. Callis, in: J.R. Lakowicz (Ed.), *Topics in Fluorescence Spectroscopy*, vol. 5, Plenum Press, New York, London, 1997, p. 1.
- [9] C.Z. Wang, C.K. Johnson, *Chem. Phys.* 179 (1994) 513.
- [10] B.W. Van Der Meer, S.-Y. Simon Chen, J.R. Lakowicz (Eds.), *Topics in Fluorescence Spectroscopy*, vol. 5, Plenum Press, New York, London, 1997, p. 145.
- [11] K.D. Belfield, M.V. Bondar, J.M. Hales, A.R. Morales, O.V. Przhonska, K.J. Schafer, *J. Fluoresc.* 15 (2005) 3.
- [12] J.R. Lakowicz, I. Gryczynski, in: J.R. Lakowicz (Ed.), *Topics in Fluorescence Spectroscopy*, vol. 5, Plenum Press, New York, London, 1997, p. 87.
- [13] M. Hamer, *The Cyanine Dyes and Related Compounds*, Interscience Publisher, New York, 1964.
- [14] A.R. Morales, *Synthesis and Characterization of New Fluorene Derivatives for Emerging Electro-optics Applications*, Ph.D. thesis, Benemerita Universidad Autonoma de Puebla, 2004.
- [15] K.D. Belfield, A.R. Morales, J.M. Hales, D.J. Hagan, E.W. Van Stryland, V.M. Chapela, *J. Percino, Chem. Mater.* 16 (2004) 2267.
- [16] J.R. Lakowicz, *Principles of Fluorescence Spectroscopy*, Kluwer Academic/Plenum Publishers, New York, 1999.
- [17] C. Xu, W.W. Webb, *J. Opt. Soc. Am. B* 13 (1996) 481.
- [18] M. Fisher, J. Georges, *Chem. Phys. Lett.* 260 (1996) 115.
- [19] J.S. Craw, J.R. Reimers, G.B. Bacskay, A.T. Wong, N.S. Hush, *Chem. Phys.* 167 (1992) 77.
- [20] P. Cronstrand, Yi Luo, H. Ågren, *Chem. Phys. Lett.* 352 (2002) 262.
- [21] V. Gaisenok, A. Sarzhevskii, *Absorption and Fluorescence Anisotropy of Complicated Molecules*, University Press, Minsk, 1986 (in Russian).
- [22] R.A. Negres, O.V. Przhonska, D.J. Hagan, E.W. Van Stryland, M.V. Bondar, Yu.L. Slominsky, A.D. Kachkovski, *IEEE J. Select. Top. Quant. Electron.*, Issue on Organics for Photonics 7 (2001) 849.
- [23] A. Streitwiser, *Molecular Orbital Theory*, Wiley, New York, London, 1963.
- [24] D. Scherer, R. Dorfler, A. Feldner, T. Vogtmann, M. Schwoerer, U. Lawrentz, W. Grahn, C. Lambert, *Chem. Phys.* 279 (2002) 179.
- [25] R.S. Lepkowitz, C.M. Cirloganu, O.V. Przhonska, D.J. Hagan, E.W. Van Stryland, M.V. Bondar, Yu.L. Slominsky, A.D. Kachkovski, E.I. Mayboroda, *Chem. Phys.* 306 (2004) 171.
- [26] W.P. Su, J.R. Schrieffer, A.J. Heeger, *Phys. Rev. B* 22 (1980) 2099.